Conformational Flexibility of Domain III of Annexin V at Membrane/Water Interfaces†

Jana Sopkova,‡ Michel Vincent,‡ Masayuki Takahashi,§ Anita Lewit-Bentley,‡ and Jacques Gallay*,‡

L.U.R.E. Laboratoire pour l'Utilisation du Rayonnement Electromagnétique, Université Paris-Sud, Bâtiment 209D, F-91898 Orsay Cedex, France, and UMR216, Institut Curie and CNRS Bâtiment 110, F-91405 Orsay Cedex, France

Received November 20, 1998; Revised Manuscript Received February 19, 1999

ABSTRACT: The conformational dynamics of domain III in annexin V bound to negatively charged phospholipid vesicles of 1-palmitoyl-2-oleoyl-*sn*-glycerophosphocholine and 1-palmitoyl-2-oleoyl-*sn*-glycerophosphoserine or incorporated into reverse micelles of water/sodium bis(2-ethylhexyl) sulfosuccinate in isooctane, used to mimic the phospholipid/water interface, was studied by steady-state and time-resolved fluorescence of its single tryptophan residue (W187). Upon interaction with sonicated phospholipid vesicles in the presence of calcium, or upon incorporation into reverse micelles without calcium, a progressive 12−14 nm red shift of the fluorescence emission spectrum of W187 is observed. The indole environment becomes therefore more polar than in the unbound protein. Three major lifetime populations describe the fluorescence intensity decays of W187 in both systems. A long-lived excited-state population characterizes the membrane-bound state of the protein. The existence of local conformers with different subnanosecond mobility is suggested by specific association between lifetimes and correlation times both for the protein in buffer and in interaction with the membrane surface. The interaction of the protein with the membrane surface preserves the existence of a rapid unhindered rotational motion, which is coupled with all three lifetimes. The longest lifetime is coupled to restricted motions in subnanosecond and nanosecond time scales. The overall amplitude of rotation of the indole ring is increased in the membrane-bound conformation of the protein. In reverse micelles, the local dynamics reported by W187 is also considerably increased whereas the overall folding of the protein remains unaffected. The same conformational change of domain III can therefore be provoked by different conditions: calcium binding at high concentration, mild acidic pH [Sopkova, J., Vincent, M., Takahashi, M., Lewit-Bentley, A., and Gallay, J. (1998) *Biochemistry 37*, 11962−11970] and the interaction of the protein with the membrane surface. The high flexibility of domain III in the membrane-bound protein suggests that this domain may not be crucial for the interaction of the protein with the membrane, in contrast with previous models. Our data are compatible with atomic force microscopy results which suggest that domain III of annexin V does not interact strongly with the membrane surface [Reviakine, I., Bergma-Schutter, W., and Brisson, A. (1998) *J. Struct. Biol. 121*, 356−361].

Annexins belong to a family of peripheral membrane proteins, which share large structural homologies and biochemical characteristics. In particular, all annexins interact with negatively charged phospholipid membranes in a calcium-dependent manner at neutral pH (*1*) and with cell membranes (*2*−*4*). To date, the exact biological function(s) of these proteins remains unknown. The propensity of these proteins to interact with model membranes and also their frequent cellular location near membrane tracts and cytoskeleton have suggested, however, that they can intervene in cellular processes implicating membrane interaction or exchange (*2*). More precisely, they can participate in physiological processes involving interaction with constituents of cellular membranes such as signal transduction (*5*), exocytosis (*6*), as regulators of phospholipase A_2 activity (*7*), or as membrane effectors (*8*) and also in the cytoskeleton as regulatory elements (9). The binding of these proteins to cellular membranes, and especially to the phospholipid bilayer, may trigger biochemical processes implying probably interactions with protein partners.

The crystal structures of many annexins are known. The analysis has been initially carried out for annexin V (*10*−*14*) and later for annexins I, II, III, IV, VI, VII, and XII (*15*−*22*). These studies show that all annexins contain a conserved core of about 300 amino acids in length, organized in a cyclic array with 4-fold repeats of 70 residues, each constituting a structural domain, with the exception of annexin VI, which contains two conserved cores. Each structural domain comprises five α-helices, wrapped into a right-handed super-helix and contains generally one principal calcium-binding site situated on the convex face of the molecule. The calcium ion is bound to carbonyl oxygens of the loop connecting helices A and B, and to a carboxyl of the negatively charged amino acid side chain (Glu or Asp) about 40 residues downstream, in the loop connecting helices D and E in the same domain. In annexin V, a particular situation prevails since the existence of the calcium-binding

† J.S. is a recipient of a postdoctoral grant from the EC (ERBBIO4-CT960083). Partial financial supports from CNRS, CEA, MESRT, and EC are acknowledged.

* To whom correspondence should be addressed. E-mail: gallay@lure.u-psud.fr.

‡ Université Paris-Sud.

§ Institut Curie and CNRS Bâtiment 110.

10.1021/bi982760g CCC: $18.00
Published on Web 04/08/1999

site in domain III requires a large conformational change to take place. This change was observed by X-ray diffraction studies (*11*, *13*, *14*), showing that the IIIA-IIIB loop is brought from a buried position onto the surface of the protein. At the same time, the position of the loop IIID-IIIE changes significantly, allowing glutamic acid 228 to approach the calcium site and to complete the calcium ligands. Interaction of the protein with the membrane occurs by its convex side, which is oriented toward the membrane surface, the calcium ions making bridges between the negatively charged headgroups of the phospholipid molecules and the binding sites on the protein. This hypothesis is compatible with the results of electron microscopy studies on two-dimensional crystals (*23*−*26*). The overall folding of the protein bound to the membrane surface does not appear to be grossly modified, but interactions between molecules must occur due to their self-association on the membrane surface (*27*).

Conformational changes of annexin V on the membrane surface have however been suggested both by calorimetry (*28*) and fluorescence studies (*29*−*35*). Two main observations were made by the latter studies which exploit the presence of the single tryptophan residue (W187) in domain III: the fluorescence intensity increased by a factor of ∼4 and the emission maximum was red-shifted by around 12−15 nm upon binding of the protein to negatively charged phospholipid membranes in the presence of calcium. This change of the emission maximum is similar to the one induced by calcium in the absence of membranes (*36*) and by mild acidic conditions (*37*, *38*), leading to the exposure of the W187 residue on the protein surface where it is more mobile (*34*, *36*, *38*).

Crystallographic studies of annexin V complexed with calcium and polar molecules such as glycerophosphoserine and glycerophosphoethanolamine have suggested that W187 was in contact in the crystal with the glycerol backbone of the glycerophosphoserine moiety (*14*). This observation was extrapolated to the real membrane bilayer situation, which led to a molecular model where W187 is in intimate contact with the first carbon atoms of the fatty acyl chains. In this putative model, the indole ring, inserted into the first carbon region of the phospholipid, should produce a restriction of the orientation and dynamics of the methylene groups. It is, however, the reverse effect that has been observed: the amplitude of motion of the first methylene groups of the phospholipid acyl chains is increased even at complete coverage of the lipid bilayer by the protein (*39*, *40*). The lateral diffusion coefficients of PC and PS molecules, measured either by excimer formation (*41*) or by fluorescence recovery after photobleaching (*39*), are considerably reduced. Therefore, the precise mode of interaction of the protein with the membrane/water interface is still not completely understood.

In this work, we addressed the question of whether the outward swinging of W187 is an important molecular step in the mechanism of interaction of annexin V with membranes. To this purpose, we investigated the influence of the association of annexin V with membrane interfaces on the dynamics of domain III. The rotational dynamics of W187 and of its environment were measured by time-resolved fluorescence intensity and anisotropy decay measurements. Two membrane model systems were used: small unilamellar vesicles of phosphatidylcholine/phosphatidylserine at different lipid/protein molar ratios (L/P) and reverse micelles of surfactant in organic solvent at different water/surfactant molar ratios. This last system provides an optically transparent experimental model of membrane/water interface, in which the proton activity and the availability of water molecules for hydration is limited (*42*, *43*).

EXPERIMENTAL PROCEDURES

Chemicals. Phospholipids (1-palmitoyl-2-oleoyl-*sn*-phosphocholine, POPC,[1] and 1-palmitoyl-2-oleoyl-*sn*-phosphoserine, POPS) were obtained from Serdary Research. Sodium bis(2-ethylhexyl) sulfosuccinate (Aerosol OT, AOT) was purchased from Sigma and used as supplied.

Protein preparation. Recombinant human annexin V was prepared as before (*44*). In this procedure, EDTA is used to remove all calcium during the purification and the protein is stored in the absence of calcium. For measurements of absorbance, circular dichroism, and fluorescence, the protein solutions were prepared in 50 mM of Tris-HCl, pH 7.5, and NaCl 0.15 M. All chemicals were of analytical grade purity and obtained from Merck, France.

Preparation of Phospholipidic Vesicles and Reverse Micelles. The phospholipid suspensions were prepared by sonication using POPC and POPS dissolved in chloroform. The organic solution was evaporated to dryness in a glass tube under a stream of nitrogen. Remaining traces of organic solvent were further removed by submitting the sample to high vacuum during several hours. Hydration of the sample was achieved with buffer, and after vortexing, the multilamellar vesicles formed were sonicated at room temperature with the micro-tip of a Branson-B12 sonicator during 5 min with half-duty cycles. The POPS/POPC molar ratio of the vesicles was varied from 10 to 25%.

Reverse micelles were prepared as previously described (*45*). Briefly, reverse micelles of AOT and water in isooctane were prepared with 0.1 M AOT and the desired amount of water. The water/surfactant molar ratios, w_0, was varied from 2.8 to 50. The total final volume of the samples was 1 mL. Solubilization of the protein (0.6 mg/mL for fluorescence and 0.15 mg/mL for far-UV CD) was achieved by sonication in a Branson-type bath sonicator for few minutes.

Steady-State Fluorescence Measurements. Tryptophan fluorescence emission spectra were recorded between 300 and 420 nm (bandwidth, 8 nm) on a SLM 8000 spectrofluorometer, using 5 × 5 mm (for the samples containing lipid vesicles) or 10 × 10 mm (for the other samples) optical path cuvettes. Blanks were always subtracted in the same experimental conditions. To remove polarization artifacts, the fluorescence emission spectra were reconstructed from the four polarized spectra as described previously (*46*). Steady-state fluorescence intensity and anisotropy excitation spectra (bandwidth, 2 nm) were performed with the same spectrofluorometer with an emission wavelength of 340 nm (bandwidth, 8 nm).

Time-resolved Fluorescence Measurements. Fluorescence intensity and anisotropy decays were obtained by the time-

[1] AOT, sodium bis(2-ethylhexyl) sulfosuccinate; EDTA, ethylenediaminetetraacetic acid; L/P, lipid/protein molar ratio; MEM, maximum entropy method; NATA, *N*-acetyl-tryptophanamide; POPC, 1-palmitoyl, 2-oleoyl-*sn*-glycerophosphocholine; POPS, 1-palmitoyl, 2-oleoyl-*sn*-glycerophosphoserine; SUV, small unilamellar vesicles; Trp, tryptophan.

correlated single photon counting technique from the $I_{vv}(t)$ and $I_{vh}(t)$ components recorded on the experimental setup installed on the SB1 window of the synchrotron radiation source Super-ACO (Anneau de Collision d'Orsay), which has already been described (*47*). Optical path cuvettes of 5 × 5 mm were used. Light scattering by the lipid vesicles was strongly reduced by interposing a 1 M $CuSO_4$ filter (1 cm optical path) on the emission side. Subtraction of the blanks without protein was systematically performed in experiments with liposomes.

Analysis of the Time-Resolved Fluorescence Data. Analyses of fluorescence intensity and anisotropy decays as sums of exponentials were performed by the maximum entropy method (see ref *48* for a review). The programs use the commercially available library of subroutines MEMSYS 5 (MEDC Ltd., U.K.). The applications of the method to fluorescence intensity and anisotropy decays have been previously published in detail for lifetime distribution (*49*) as well as for rotational correlation time distribution (one-dimensional analysis) and for the coupling between lifetimes τ and rotational correlation times θ (two-dimensional analysis) (*46*). In this last analysis, the $\Gamma(\tau,\theta)$ coefficient represents the relative proportion of the population of chromophore with lifetime τ and rotational correlation time θ in the expression of the polarized fluorescence decays:

$$I_{vv}(t) = \int_0^\infty \int_0^\infty \Gamma(\tau,\theta)\, e^{-t/\tau}(1 + 2A\, e^{-t/\theta})\, d\tau d\theta \quad (1)$$

$$I_{vh}(t) = \int_0^\infty \int_0^\infty \Gamma(\tau,\theta)\, e^{-t/\tau}(1 + A\, e^{-t/\theta})\, d\tau d\theta \quad (2)$$

where A is the intrinsic anisotropy.

In principle, such an analysis allows the description of lifetime heterogeneity and the detection of the possible association between one particular excited-state lifetime of the fluorophore and its rotational correlation time. There is nevertheless an inherent limit to this method, since the parallel and the perpendicular components of the polarized decay involve in their expressions an harmonic mean κ_i between τ_i and θ_i:

$$1/\kappa_i = 1/\tau_i + 1/\theta_i \quad (3)$$

where τ_i and θ_i can be exchanged without any modification in the κ_i value, leading to construction of iso-κ curves.

Calculations were performed on a DEC Alpha computer Vax 7620. The program including the MEMSYS 5 subroutines was written in double precision FORTRAN 77. A total of 150 lifetime values was used for the fluorescence intensity decay analysis, and 100 rotational correlation time values were used for polarized decay analysis. The global analysis of $I_{vv}(t)$ and $I_{vh}(t)$ was performed with 40 values, respectively, for τ and θ.

Orientational order parameter and semiangle of the wobbling cone of the indole ring rotation were calculated according to Kinosita et al. (*50*).

Circular Dichroism Measurements. CD spectra were measured with a J-710 spectropolarimeter (Jasco, Japan) at room temperature (22 °C). The bandwidth was 2 nm, and the spectra were averaged over 10 scans of 100 nm/min with integration time of 0.5 s. The spectra were measured in a 0.1 cm optical path cuvette. Protein concentration of ~2 μM (0.15 mg/mL) was used.

RESULTS

The Interaction of Annexin V with SUV Modifies the Polarity of the W187 Environment: Steady-State Fluorescence Intensity Measurements. Binding of annexin V to negatively charged phospholipid membranes depends on the concentration of calcium at neutral pH (*1*, *2*). The binding of the protein to SUV was examined by performing a "two-dimensional" titration (changes of phospholipid and calcium concentrations) of the three-component system, annexin-calcium-phospholipid vesicles, by steady-state fluorescence measurements. We estimated the concentration of calcium and phospholipids corresponding to the saturation of this complex at a given concentration of annexin V and a mole fraction of POPS/POPC of 20% in the vesicles. A first titration measured the change of the fluorescence emission spectrum of W187 provoked by the addition of SUV at a concentration of annexin V of ~10 μM and a calcium concentration of 0.5 mM. At this concentration, calcium does not exhibit any effect on the fluorescence spectrum of annexin V in the absence of phospholipids. The addition of SUV induces a saturatable red-shift from 325 nm to about 335 nm for a concentration of phospholipids of 8.5 10^{-4} M (L/P = 85), above which the emission maximum remains at a constant value (Figure 1A). A second titration was performed with $CaCl_2$. The sample contained the same concentration of protein and 1.5 mM phospholipids (L/P = 150). The calcium titration induced a red-shift from 325 to 342 nm (Figure 1B), comparable in magnitude to that previously published (*29*, *34*). As compared to the spectral shift induced by calcium ions alone, the average midpoint of the titration is decreased by about 1 order of magnitude in the presence of SUV (5−6 mM in the absence and 0.5 mM in the presence of SUV).

The influence of the vesicle composition was checked to obtain accurate information about the interaction and to minimize the aggregation of the protein−vesicle complexes, which may occur at high concentrations of both calcium and phospholipids. This aggregation results in strong light scattering, which may interfere with the anisotropy decay measurements, especially at short times. We observed that the half-maximum saturation of the red-shift was occurring at similar concentrations: 1.8 mM for 25% POPS, 2.3 mM for 20% POPS, and 2.8 mM for 10% POPS, in conditions of lipid/protein molar ratio = 54. The aggregation was smaller at 10 and 20% than at 25% POPS. We therefore used a POPS/POPC molar ratio of 20% for time-resolved experiments.

The Interaction of Annexin V with SUV Affects the Local Conformation around W187: A Fluorescence Lifetime Study. The fluorescence emission decay of W187 in annexin V in the absence of calcium and of phospholipid vesicles is not monoexponential. MEM analysis describes the decay with three excited-state lifetime populations (Figure 2A), in agreement with previously published data (*34*−*36*). Decay-associated spectra measurements show that the two major lifetimes remain invariant through the emission spectrum. Both populations display an emission maximum at around 320−325 nm, as the steady-state fluorescence emission spectrum (data not shown).

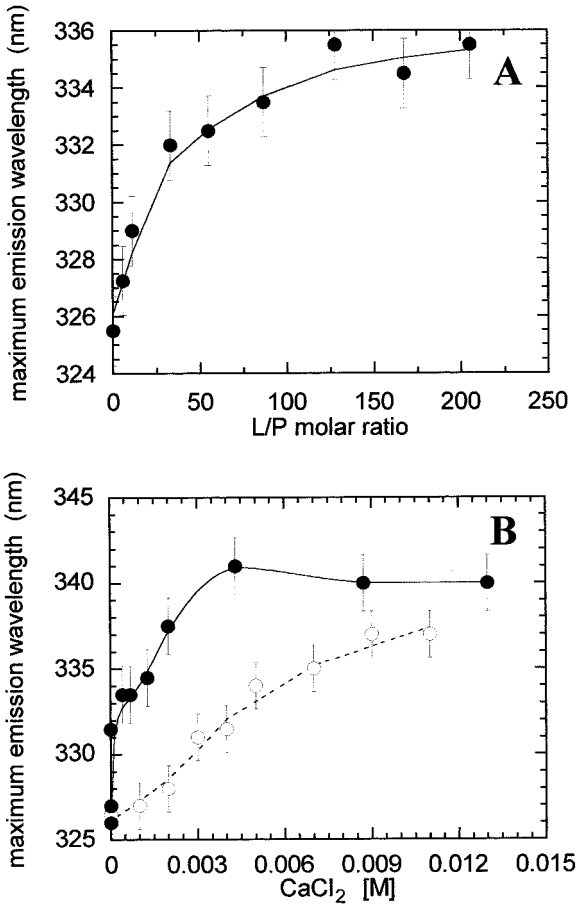

FIGURE 1: (A) Variation of the maximum emission wavelength of W187 of annexin V as a function of the phospholipid concentration (POPC/POPS 80:20 M/M). Protein concentration, 10 μM; $CaCl_2$ concentration, 0.5 mM. Excitation wavelength, 295 nm (bandwidth, 2 nm). (B) Variation of the maximum emission wavelength of W187 as a function of the concentration of $CaCl_2$. (●) In the presence of SUV (POPC/POPS 80:20 M/M) corresponding to 1.5 mM phospholipids. (○) In the absence of phospholipids. Annexin V concentration, 9.7 μM.

In the presence of 10 mM calcium, already inducing a shift of 12 nm (Figure 1B), the lifetime profile is also modified (Figure 2B). Three lifetime populations are still detectable but the center of each peak is shifted to longer values and the longest-lived excited-state becomes dominant. The effect is similar to that observed at higher calcium concentrations (*36*). This change of lifetime distribution indicates that the interactions of the indole ring with proximate quenching groups occurring in its hydrophobic pocket in the absence of calcium are suppressed for a large part due to a partial exposure of the indole ring at the protein surface. One of these groups is likely the peptide bond involving Thr224, which is H-bonded to the nitrogen atom of the indole ring.

The interaction of the protein with SUV containing POPS/POPC at a mole fraction of 20% further modifies the excited-state lifetime profile (Figure 2, panels C−E). At the lowest point of L/P ratio, where the saturation of the protein by lipid vesicles is obviously not complete (Figure 2C), the three shortest lifetime populations are similar to that of the free protein without calcium, whereas a long-lived lifetime species appears. It seems that in these low L/P values, we may deal with a weight sum of the lifetime components of the "free" and "bound" protein lifetime spectra.

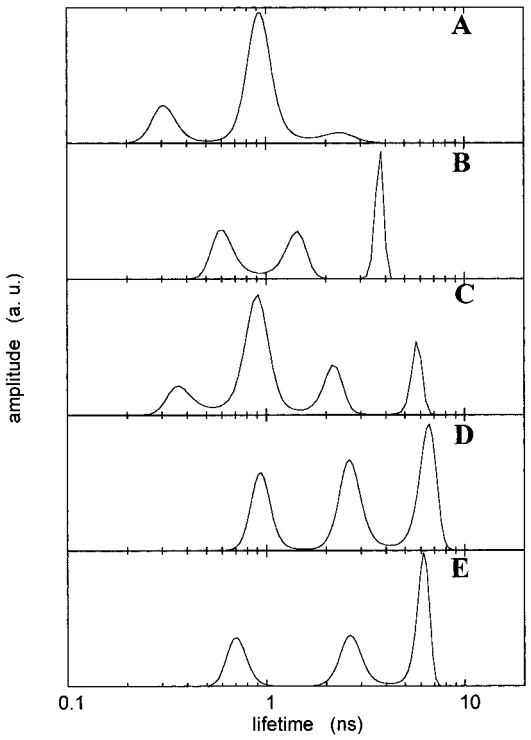

FIGURE 2: Excited-state lifetime distributions of W187 at different lipid/protein molar ratios (L/P). (A) L/P = 0, $CaCl_2$ = 0; (B) L/P = 0, $CaCl_2$ = 10 mM; (C) L/P = 59, $CaCl_2$ = 4 mM; (D) L/P = 76, $CaCl_2$ = 13 mM; (E) L/P = 143, $CaCl_2$ = 10 mM; (F) L/P = 730, $CaCl_2$ = 10 mM. In all measurements the excitation wavelength was set at 295 nm (bandwidth, 4 nm), the emission wavelength was 325 for panel A and 340 nm (bandwidth, 8 nm) for the other measurements. Protein concentration, 10 μM. Temperature, 20 °C.

The progressive red shift of the W187 fluorescence emission spectrum as a function of the L/P ratio is accompanied by the gradual appearance of the long excited-state lifetime of ~6 ns (Figure 2, panels C−E, and Figure 3B). The increase of the proportion of this long lifetime starts at the lowest L/P ratio we have tested (L/P = 27) and levels off at L/P ≈ 200 (Figure 3B). The proportion of the major excited-state lifetime population in the free form of the protein (center ≈ 1 ns), remains first constant up to a L/P ratio of 50 and then decreases by one-half to reach approximately a plateau for a L/P ratio of about 150 (Figure 3B). The number of peaks reduces to three at higher L/P ratios where the shortest lifetime population disappears. At the highest L/P ratios, the two longest lifetimes dominate the fluorescence decay (about 75% of the excited-state populations and 95% of the fluorescence intensity). The mean excited-state lifetime increases regularly by a factor of ~4 until a L/P ratio of ~150 (Figure 3A), in similar proportion as the steady-state fluorescence intensity (Table 1).

Time-resolved acrylamide quenching experiments were represented as Stern−Volmer plots for the longer and intermediate lifetimes. The K_{sv} constants are, respectively, 0.93 and 1.13 M^{-1}, allowing the calculation of a bimolecular quenching constant k_q of $(1.7-2) \times 10^8$ M^{-1} s^{-1}, comparable to that measured for the membrane-free protein. It is much lower than that measured in the presence of calcium or at pH 4 (*38*). This value corresponds to a low accessibility of the indole ring to the quencher (*51*), despite its red-shifted emission.

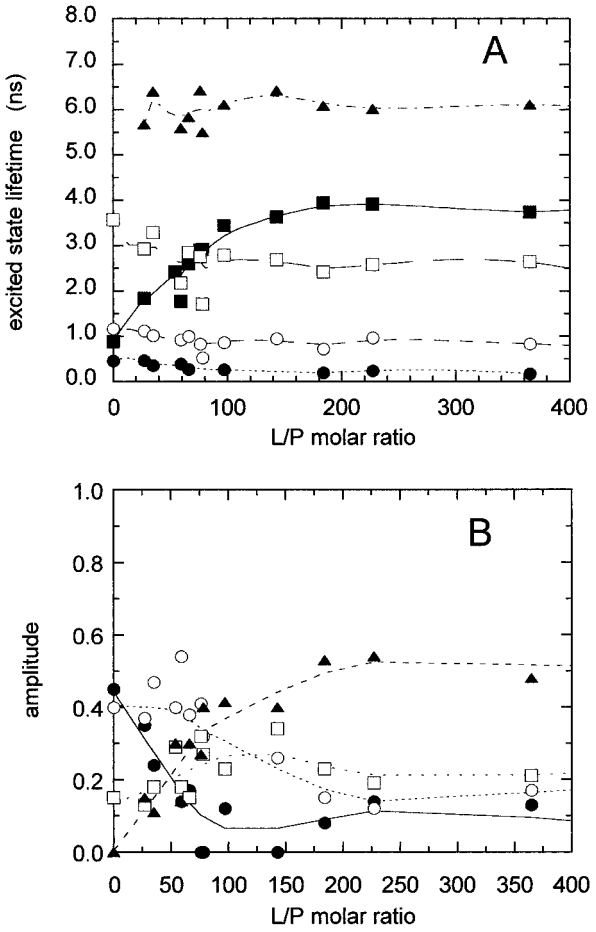

FIGURE 3: (A) Variation of the excited-state lifetime values (barycenter of each lifetime peak) as a function of the L/P ratio (POPC/POPS 80:20 M/M). (●) τ_1; (○) τ_2; (□) τ_3; (▲) τ_4; (■) $<\tau>$. (B) Variation of the amplitude values C_i (normalized areas) of each lifetime population as a function of the L/P ratio. (●) C_1; (○) C_2; (□) C_3; (▲) C_4. The mean lifetime $<\tau>$ was calculated as $<\tau> = \Sigma C_i\tau_i$.

The Mobility of W187 Is Modified after Interaction of Annexin V with SUV: Steady-State and Time-Resolved Fluorescence Anisotropy Study. The rotational dynamics of W187 when the protein is bound to phospholipid membranes has never been measured. A convenient way to perform these experiments is to measure the steady-state anisotropy value as a function of the excitation wavelength since the indole chromophore displays characteristic spectroscopic features allowing to discriminate between motional effects and energy transfer effects (*52*, *53*). The latter process can be present since one possibility of organization of the aggregates on the membrane surface may involve contacts between domains III (*25*, *27*).

The steady-state fluorescence anisotropy excitation spectrum of free annexin V, measured at the maximum emission wavelength (325 nm), shows high anisotropy values whatever the excitation wavelength (Figure 4). This is a characteristic feature of a quasi-immobilized Trp with a short mean excited-state lifetime (the mean lifetime/mean correlation time ratio is small). We observe the characteristic minimum of the Trp anisotropy excitation spectrum near 290 nm and a steep increase at excitation wavelengths ranging from 290 to 300 nm. The anisotropy value at 305 nm is between 0.25 and 0.30, close to the maximum value measured in vitrified medium in the absence of motion both for NATA and bis-tryptophan (*53*, *54*).

Addition of calcium in the millimolar concentration range leads to only a small change of the fluorescence excitation spectrum and a slight decrease of the anisotropy values (Figure 4). By contrast, binding to SUV containing POPS/POPC (20%) at a high L/P ratio of 500 enhances the characteristic shoulder observed on the fluorescence excitation spectrum at 290 nm, which becomes a peak. This is due to the enhancement of the fluorescence quantum yield of W187 with respect to tyrosine residues. The anisotropy values decrease considerably throughout the whole excitation spectrum. This indicates either that W187 becomes more mobile or that the mean excited-state lifetime becomes longer or both. Time-resolved measurements show that both effects are present. Resonant energy transfer between Trp(s) of different annexin V molecules on the membrane is not likely since, in the red edge of the excitation spectrum ($\lambda \geq 300$ nm), the anisotropy spectrum lies always below that of the unbound protein.

The rotational motion of the indole ring can be monitored directly by time-resolved anisotropy decay experiments. The fluorescence polarized decay data can be analyzed using two models: a one-dimensional model, which correlates all the excited-state lifetimes with all the rotational correlation times, and a two-dimensional model, which does not assume any a priori specific coupling between these parameters.

In the absence of calcium and membranes, the first analysis does not reveal any fast rotational motion of the indole ring (Table 1). Only the presence of the Brownian motion of the monomeric protein is detected. In the presence of 10 mM $CaCl_2$, a nanosecond rotational motion with large amplitude is detectable (Table 1). In the presence of POPC/POPS SUV at low L/P molar ratios and 10 mM calcium, this motion is preserved and an infinite component is observed. The wobbling angle of the rotational motion of the indole ring is reduced as compared to the value in the presence of calcium only, but it is much larger than the value in the protein alone (Table 1). This wobbling angle value is further increased at higher L/P ratios and additional correlation times appear. It should be remarked that in all cases the initial anisotropy value is always smaller than that expected for an immobile Trp residue at this excitation wavelength (*53*).

The two-dimensional analysis of the fluorescence-polarized decays for the protein in the absence of membranes and calcium shows the existence of a subnanosecond rotational motion that was not observed in the one-dimensional analysis (Figure 5A). This is likely due to the coupling of the minor shortest-lived excited state with this fast rotational motion describing the rotational motion of the indole ring (Figure 5A) as observed recently (*38*). It should be remarked that if the short-lived excited-state population were also associated with the Brownian rotation of the protein, this would have appeared as an infinite anisotropy value since the lifetime value (~300 ps) is much shorter than the Brownian rotational correlation time value. This short lifetime corresponds therefore to a conformer where the indole ring rotation is isotropic (with no steric hindrances). The major excited state of 0.9 ns, in contrast, is associated more with the Brownian motion of the protein than with the internal rotation of the indole ring. It corresponds likely to a conformer where the subnanosecond rotation of the indole ring is largely hindered.

Table 1: Fluorescence Intensity and Anisotropy Decay Parameters for W187 in Annexin V in Neutral Buffer, pH 7.5, in the Presence of 10 mM $CaCl_2$ without Membranes and as a Function of the Lipid/Protein Molar Ratio (Experimental Conditions as in Figure 2)[a]

lipid/protein ratio M/M	τ_1 (ns) C_1	τ_2 (ns) C_2	τ_3 (ns) C_3	τ_4 (ns) C_4	$<\tau>$ (ns)	θ_1 (ns) β_1	θ_2 (ns) β_2	θ_3 (ns) β_3	$A_{t=0}$	S	ω_{max}
0	0.32	0.95	2.67		0.94			14.9	0.174	0.93	17
	0.20	0.72	0.07					0.174			
+0.01 M	0.46	1.18	3.57		1.23		3.4	29.8	0.160	0.89	46
$CaCl_2$	0.45	0.40	0.15	0.15			0.089	0.071			
+0.1 M $CaCl_2$	0.74	1.91	4.09		2.17	0.08	1.20	13.1	0.244	0.75	35
	0.39	0.28	0.33			0.106	0.073	0.065			
L/P = 27	0.46	1.18	2.93	5.68	1.84		2.9	∞	0.155	0.75	35
	0.35	0.37	0.13	0.15			0.043	0.112			
L/P = 54	0.55	1.68		5.39	2.42	1.7	7.5	∞	0.152	0.69	39
	0.40	0.29		0.31		0.035	0.022	0.095			
L/P = 78	0.52	1.71		5.50	2.92	0.5	4.5	∞	0.164	0.74	36
	0.33	0.27		0.40		0.027	0.028	0.109			
L/P = 342	0.45	1.76		5.68	3.50	3.2	18.0	∞	0.130	0.64	43
	0.22	0.26		0.52		0.012	0.037	0.081			
L/P = 730	0.72		2.70	6.08	3.68	5.7		∞	0.100	0.59	46
	0.26		0.30	0.44		0.030		0.070			

[a] Excitation wavelength: 295 nm (bandwidth, 4 nm), emission wavelength: 340 nm (bandwidth, 8 nm) except for the protein at neutral pH in the absence of calcium (325 nm). The mean lifetime $<\tau>$ was calculated as $<\tau> = \Sigma C_i\tau_i$. C_i are the relative areas of the lifetime peaks. The anisotropy analyses were performed with the one-dimensional model using a sum of exponentials: $A(t) = \sum_i \beta_i \exp(-t/\theta_1)$. The order parameter was calculated from $\beta_{3i}A_0 = S^2$ (with $A_0 = 0.2$) (*53*). The semiangle of the wobbling cone ω_{max} was calculated according to Kinosita et al. (*50*) as $S^2 = [1/2 \cos \omega_{max} (1 + \cos \omega_{max})]^2$.

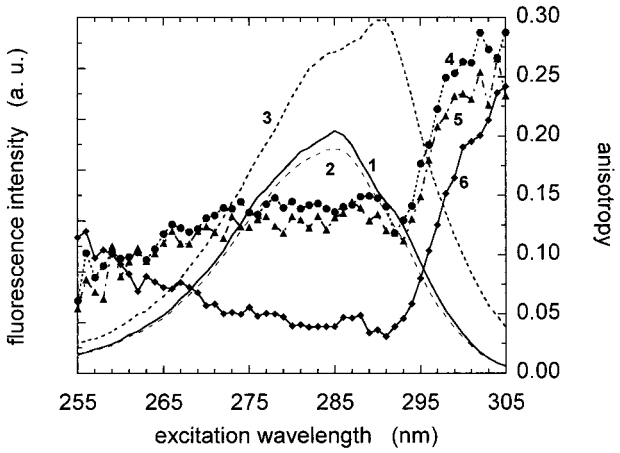

FIGURE 4: Steady-state fluorescence excitation spectra of (1) annexin V in neutral buffer, pH 7, (2) annexin V in the presence of 5.5 mM $CaCl_2$, and (3) in the presence of 5.5 mM $CaCl_2$ and with a L/P ratio of 500. Steady-state anisotropy excitation spectra of (4) annexin V in neutral buffer, (5) annexin V in the presence of 10 mM $CaCl_2$, and (6) in the presence of 5.5 mM $CaCl_2$ and with a L/P ratio of 500. Protein concentration, 4.5 μM. Emission wavelength, 325 nm for calcium-free and calcium-bound annexin V, 340 nm for membrane-bound annexin V. Temperature, 20 °C.

The presence of 10 mM calcium slightly affects the local dynamics in such a way that the proportion of the conformer which displays a fast mobility of the indole ring is increased (Figure 5B). This feature allows the observation of the fast depolarization motion in the one-dimensional analysis (Table 1).

The two-dimensional analysis of the polarized decays of the membrane-bound protein shows also the existence of specific coupling between lifetime and correlation times (Figure 5C). A fast rotation of 200−400 ps affects all the lifetime populations. At low L/P ratios (L/P = 35 and 54), the shortest lifetime is also associated with an infinite component while this is not the case at high L/P ratios (Table 2). This indicates the existence of rotational constraints occurring at high protein concentrations on the membrane that are released when the protein is diluted on the membrane surface at low protein concentration. At L/P = 730, the shortest lifetime is associated only with this fast rotational correlation time, while the long lifetime is coupled both to this fast rotation, to an intermediate motion (5 ns), and to an infinitely long correlation time (Figure 5C and Table 2). The short lifetimes correspond therefore to conformers where the indole rotation is isotropic, while the long lifetime corresponds to a conformer where the indole rotation is restricted by steric hindrances. This conformer is also sensitive to slower protein flexibilities that are still present on the membrane surface. The Brownian rotational correlation time is extremely long as compared to the lifetime because the protein is firmly bound to the large rotating body constituted by the lipid vesicle, the size of which corresponds to a tumbling motion of the order of microseconds.

The Interaction of Annexin V with Reverse Micelles: Changes in the W187 Environment as Probed by Steady-State Fluorescence Spectrum and Excited-State Lifetime Distribution. The binding of annexin V to phospholipid membranes at neutral pH is classically depicted as mainly driven by electrostatic interactions involving calcium ions, which maintain the protein at the membrane surface (*14*). The protein convex surface is most likely in contact with the first water layers surrounding the phospholipid polar headgroups that constitute the interface of the membrane with the aqueous solvent. In this interfacial water layer region, the proton activity as well as the availability of water molecules for hydration is significantly modified (*42*). Reverse micelles can be used to mimic this interfacial region and its influence on protein conformation and dynamics. These microemulsions can solubilize many proteins of different kinds (*42*, *43*, *45*, *55*, *56*). They display convenient properties for optical studies (for a recent review see ref *57*).

In the micromolar concentration range, annexin V is soluble in reverse micelles formed by the surfactant AOT in isooctane at a water/surfactant molar ratio (w_0) as low as 2.8 as judged by the absorption spectrum which did not exhibit any light scattering (data not shown). At this low water content, the fluorescence emission maximum is already red-shifted by about 12 nm with respect to the protein in buffer solution at neutral pH (Figure 6). The fluorescence

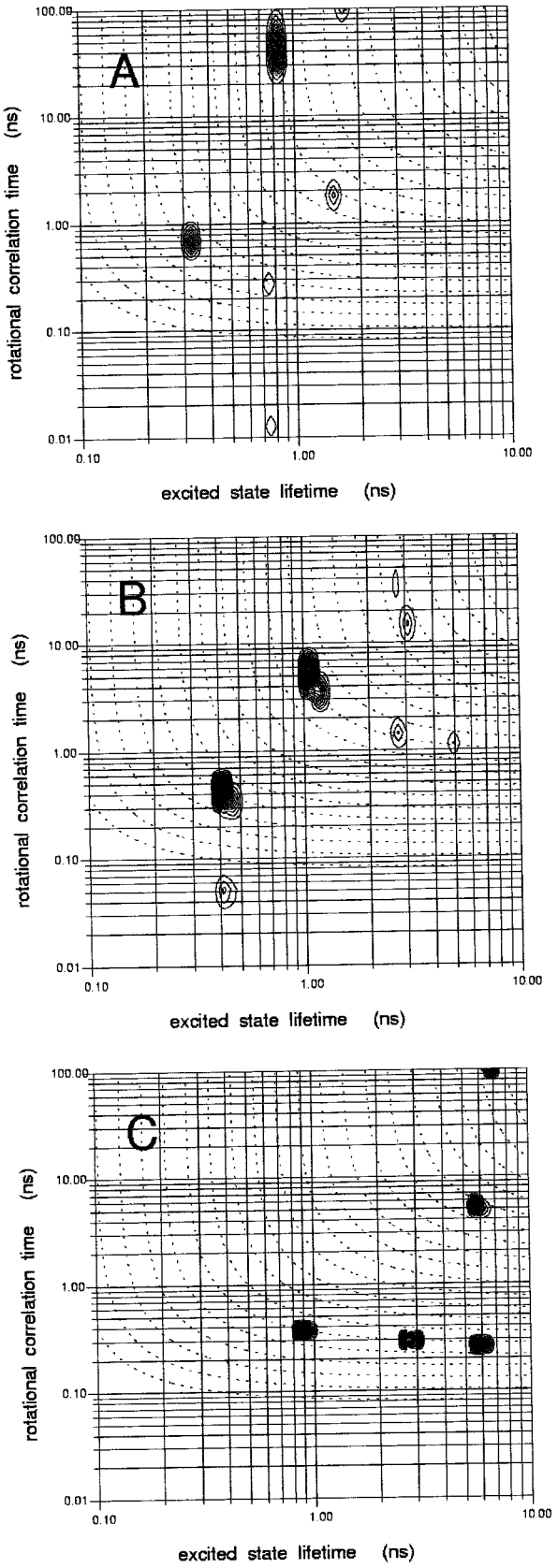

FIGURE 5: MEM reconstructed $\Gamma(\tau, \theta)$ distributions of (A) annexin V in neutral buffer, (B) annexin V in neutral buffer with 10 mM $CaCl_2$, and (C) in the presence of SUV (POPC/POPS 80:20) at a lipid/protein molar ratio of 730 and 10 mM $CaCl_2$. Protein concentration, 10 μM. Dashed lines represents the iso-κ curves defined in the Materials and Methods.

Table 2: Distribution of the $\Gamma(\tau, \theta)$ Parameters of the Polarized Fluorescence Decays of W187 at Different Lipid/Protein Molar Ratios[a]

	τ(ns)			
θ(ns)	0.4	1.1	2.9	5
0.05−0.5	0.42			
1.5−5		0.41	0.05	
8−20			0.09	0.03
L/P = 35				

	τ(ns)			
θ(ns)	0.7	1.7	4.2	7.3
<0.02	0.22			
0.4−1.8	0.21	0.23	0.08	0.06
10−20			0.07	
∞	0.08		0.04	0.01
L/P = 54				

	τ(ns)		
θ(ns)	0.6	1.7	5.2
0.1	0.30		
1.5−4		0.29	0.08
15			0.18
∞	0.13		0.02
L/P = 342			

	τ(ns)		
θ(ns)	0.5	1.8	5.4
0.05	0.33	0.03	0.04
1.5−2		0.20	0.10
30			0.19
∞			0.10
L/P = 730			

	τ(ns)		
θ(ns)	0.9	2.8	6.0
0.3−0.4	0.26	0.26	0.14
5−6			0.21
∞			0.13

[a] $CaCl_2$ concentrations as in Figure 2. No lipids, $CaCl_2$ 10 mM.

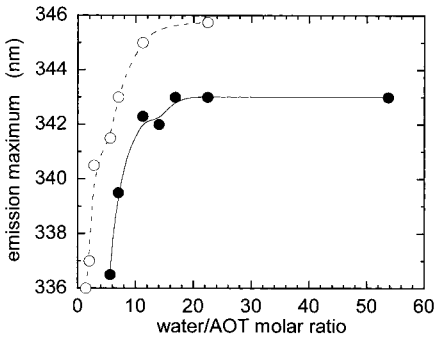

FIGURE 6: Variation of the maximum emission wavelength of W187 of annexin V (●) and of NATA (○) incorporated into reverse micelles of water/AOT in isooctane as a function of the water/surfactant molar ratio w_0. Protein concentration 2.5 μM for w_0 = 2.8 and 10 μM for the others w_0. Excitation wavelength, 295 nm.

emission maximum is sensitive to the water content of the micelles. It is more and more shifted to the red with increasing water content of the reverse micelles (Figure 6). Its value culminates at 343 nm ($\Delta\lambda_{max}$ = 17 nm) for a w_0 value of ~15 whereafter it stays at a constant value. Data for NATA are presented for comparison. The maximum of emission of this Trp derivative is always larger than that of

Table 3: Fluorescence Intensity and Anisotropy Decay Parameters of W187 in Annexin V Incorporated into Reverse Micelles as a Function of the Water/AOT Molar Ratio (w_0)[a]

water/AOT molar ratio w_0	τ_1 (ns) C_1	τ_2 (ns) C_2	τ_3 (ns) C_3	τ_4 (ns) C_4	$<\tau>$ (ns)	θ_1 (ns) β_1	θ_2 (ns) β_2	θ_3 (ns) β_3	θ_4 (ns) β_4	$A_{t=0}$	S	ω_{max}
5.6	0.19	1.28	3.14	6.12				1.9	61	0.143	0.76	34
	0.30	0.30	0.35	0.05	1.86			0.027	0.116			
11.2	0.13	0.82	2.19	4.52		0.1	0.8	7.1	35.6	0.206	0.58	46
	0.25	0.29	0.38	0.08	1.46	0.062	0.026	0.050	0.068			
16.8	0.41	1.47	3.30			0.17	0.7	2.6	22.3	0.193	0.61	45
	0.28	0.47	0.25		1.65	0.058	0.013	0.047	0.075			
22.4	0.22	0.93	2.22	4.56		0.08	0.5	2.9	26.1	0.17	0.60	46
	0.26	0.28	0.39	0.07	1.48	0.027	0.023	0.058	0.071			

[a] Excitation wavelength, 295 nm (bandwidth, 4 nm); emission wavelength, 335 nm (bandwidth, 8 nm). The mean lifetime $<\tau>$ was calculated as shown in Table 1. The analyses of the anisotropy were performed with the one-dimensional model. The order parameter S was calculated from $\beta_4/0.2 = S^2$, and the semiangle of the wobbling cone ω_{max} was obtained according to Kinosita et al. (*50*).

the W187 in annexin V, and it saturates at higher emission wavelength values. These observations suggest that the conformational change of domain III of annexin V does occur in these microemulsions. This leads to a partial exposure of the W187 residue to the aqueous solvent pool of reverse micelles. A complete exposure would lead to a maximum emission wavelength identical to that of NATA, as has been found for ACTH (1−24) (*45*).

The fluorescence emission decay of W187 is also modified when the protein is dissolved into reverse micelles. Four well-separated excited-state lifetime populations are detected (Table 3). This large heterogeneity suggests the existence in these systems of large conformational dynamics in the slow time scale with respect to these lifetimes. The proportion of the major lifetime of ~0.9−1 ns, which characterizes W187 emission in the protein in buffer at neutral pH, is strongly decreased when the protein is included into the reverse micelles. The proportion of a longer lifetime (3 ns) is enhanced from few percent to 35−40% whatever the aqueous content of the micelles (Table 3). These modifications of the W187 lifetime distribution show that the conformation of domain III is considerably changed in these interfacial systems in a similar way as in the membrane-bound protein.

The Mobility of W187 Is Modified after Incorporation of Annexin V into Reverse Micelles: Time-Resolved Fluorescence Anisotropy Study. The subnanosecond and nanosecond rotations of the indole ring in annexin V incorporated into reverse micelles are strongly increased. The analysis of the polarized fluorescence decays by the one-dimensional anisotropy model shows the existence of two or more rotational correlation times in the picosecond−nanosecond time range (Table 3). The values of the orientational order parameter of the subnanosecond rotation (S) are significantly lower and the values of the wobbling angle of rotation of the indole ring (ω_{max}) are higher at all w_0 than those calculated for the protein in neutral buffer (Tables 1 and 3). The local motion of the W187 residue is of larger amplitude in the reverse micelles, a situation similar to that observed for the protein bound to negatively charged membranes. The amplitude of internal rotation estimated by ω_{max} increases when the w_0 value increases from 5.6 to 11.2 and then remains at a constant value. The two-dimensional analysis does not reveal a specific association between lifetimes and correlation times: all the rotations affect all the lifetime populations (data not shown).

Secondary Structure of Annexin V in Reverse Micelles Assessed by Circular Dichroism. The overall secondary structure of the protein is not significantly modified upon incorporation into reverse micelles at different water/surfactant molar ratios as assessed from the dichroic bands characteristic of the α-helical structure (Figure 7).

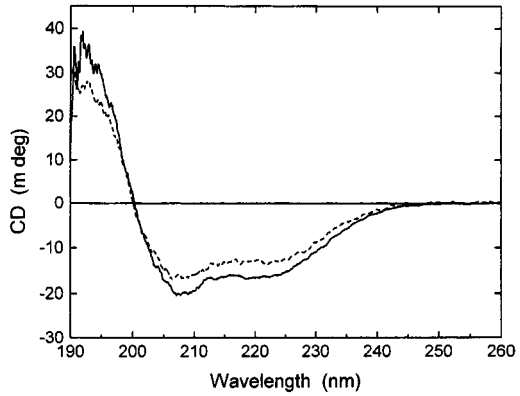

FIGURE 7: Circular dichroism spectra of annexin V incorporated in reverse micelles of water/AOT in isooctane at two water/surfactant molar ratio w_0 (dotted line, $w_0 = 5.6$; full line, $w_0 = 22.4$).

DISCUSSION

A number of studies have focused on the understanding of the mechanism of the interaction of annexins with pure phospholipid model membranes in order to define the mechanism of their potential physiological function(s) at the molecular level (for a recent review, see ref *1*). The 3D-structure of annexin molecules in increasing number has allowed the comparison with other interfacial proteins such as phospholipases, which require calcium as a cofactor for binding to membranes (*58*). This led to the observation that the consensus sequences and the structure of the calcium-binding sites of annexin V share high similarities with the single calcium site of phospholipase A_2 (*59*). Nevertheless, the annexin calcium-binding sites are highly exposed on the surface of the molecule, while that of phospholipase A_2 lies within the enzymatic site cavity, which suggests that the mode of interaction with phospholipids will be different.

On the basis of crystal studies using isolated polar headgroups (glycerophosphoserine and glycerophosphoethanolamine) as phospholipid analogues, a model of annexin V/membrane interaction was proposed (*14*). In this model, domain III of the protein participates directly in the interaction with the membrane via its calcium-binding site and the W187 residue. This can occur only if the protein changes its overall concave shape: it should become more flat on

the membrane surface (*26*). Following suggestions obtained by fluorescence of W187 (*31*), the model proposes that the protein binds to the membrane interface not only by calcium bridges but also by hydrophobic interactions between phospholipid molecules and the side-chain of the W187 residue. In the membrane-bound conformation of the protein, the indole ring protrudes out of the protein surface, in a similar way as in the high calcium structure (*10*, *11*, *13*). In this model, the aromatic side chain is located in close contact with the first methylene groups of the fatty acid chains (*14*).

On the basis of this model, we can predict several features. First, the hydrophobic interactions between the indole ring and the acyl chains should be substantial. Second, a large change of polarity of the local environment of W187, which should be reflected in its fluorescence properties, should be observed. Third, if the indole ring is indeed inserted in the membrane bilayer at the level of the first methylene groups of the fatty acid chains, it should restrict their dynamics. Finally, the mobility of W187 should also be strongly affected.

Concerning the first point, if the Trp residue is involved in any hydrophobic interaction, their energy is insufficient for tight binding to phospholipids, otherwise the protein would interact with zwitterionic phosphatidylcholine membranes (*32*) and its binding to negatively charged membranes would not be reversible by the addition of EDTA (*29*).

Calorimetric measurements also provide experimental arguments arguing against the existence of hydrophobic interactions of substantial amplitude involved in the stabilization of the annexin V-calcium-membrane complex. Calcium binding either to the protein or to the negatively charged phospholipid molecules does not result in a large enthalpy change (about 3 kcal for one calcium site). The free energy of interaction (ΔG), estimated from the saturation curve of annexin V by calcium without membranes, is around 3 kcal mol^{-1}. Therefore, the protein−calcium interaction occurs with no entropy changes, which suggests that calcium binding and the corresponding conformational change of domain III involve electrostatic interactions mainly, in agreement with the recently observed pH effect on the conformational stability of domain III (*37*, *38*). Interaction of the protein with membranes occurs with an apparent dissociation constant in the nanomolar concentration range, as estimated from the data of saturation of vesicles by the protein (*34*). This leads to a value of ΔG of interaction of $\sim$12 kcal mol^{-1}. A large enthalpy of binding of the protein on the membranes has been directly measured ($\Delta H_{binding} \approx 25$ kcal mol^{-1}) (*28*). Therefore, the calcium-mediated binding of annexin V to the membrane vesicles results in only small entropy changes. This suggests that the annexin V−membrane interaction does not involve strong hydrophobic interactions. The large ΔH of binding of the protein to the membrane can be due in part to the associated conformational change of domain III and to membrane lipid reorganization (*28*).

Moreover, if hydrophobic interactions involving W187 were occurring, the fluorescence emission spectrum should be blue-shifted with respect to that of the W187 exposed conformation when calcium ion is bound to domain III. Only a weak spectral shift is however observed for the protein bound to the membrane as compared to the unbound protein at the same calcium concentration (10 mM). The maximum of the fluorescence emission stays at 338−340 nm, similar to values found for Trp at the membrane/water interface in model peptides (*60*). Moreover, a similar value of the maximum of fluorescence emission of W187 has been reported recently in moderately acidic pH conditions in the absence of membranes (*37*, *38*). A similar effect is observed in the present work in reverse micelles in the absence of calcium.

The large increase in quantum yield upon protein binding does not give support to the existence of these interactions either. There is, in principle, no correlation between high quantum yield values and blue fluorescence emission or conversely, between low quantum yield and red emission of indole. While the energy distribution of the photons (the emission spectrum) is sensitive to dipolar interactions in the excited state (or local electric field), the quantum yield depends on the respective efficiencies of the radiative and nonradiative processes. External quenching efficiency is increased by the presence of electron scavengers such as disulfide bridges for instance, peptide bonds or protonated amino acid side chains, in the close environment of the indole ring (see ref *61* for a recent review). There is no contradiction, in fact, between the increase of quantum yield and the red-shift of the fluorescence emission spectrum. The increase in quantum yield of the Trp-exposed conformation with respect to the Trp-buried conformation can be explained by the suppression of the quenching interactions, which originate from tertiary contacts between the W187 indole ring and close protein moieties in the former conformation.

Another experimental argument in contradiction with the existence of hydrophobic interactions involving the W187 residue in domain III arose recently from studies of point mutants constructed in the calcium-binding sites of each domain of the protein. Specific disturbing effects on the propensity of the protein to bind to negatively charged phospholipidic membranes were observed (*40*). The removal of the acidic amino acid involved in the calcium-binding site of domain III (mutation E228A) left the fluorescence intensity titration curve as a function of calcium concentration surprisingly unchanged. The replacement of E72 in domain I by Q or of D144 in domain II by N resulted in a strong decrease of annexin V binding efficiency to the membranes, whereas mutation of domain IV (D303N) did not change the binding (*40*).

With respect to the effect of the protein on the phospholipid dynamics, the results of ^{2}H NMR are the opposite of what is expected, since a decrease of the order parameter of this part of the acyl chain has been observed (*39*, *40*). This can be interpreted as resulting from a reduction of intermolecular interactions between phospholipid headgroups produced by annexin V binding. Annexin V appears to behave as a "spacing" agent of the lipid packing. No effect of annexin V binding on the phosphorus order parameter of PC molecules has been found by ^{31}P NMR, which indicates that the orientation and motion of the PC headgroups remain unperturbed by the protein (*40*). Earlier ^{31}P NMR studies (*62*) do not unfortunately provide information on this point since the authors had been working on small vesicles which lead to dynamic averaging of the phosphorus chemical shift anisotropy.

These observations are therefore difficult to reconcile with the insertion of a moiety of the size of indole between the lipid molecules at the level of the first methylene groups or

near the glycerol backbone in the membrane bilayer where the packing constraints are the highest.

Several data in the literature have nevertheless been interpreted as supporting the hypothesis of hydrophobic interactions involving the indole ring of W187 of annexin V and phospholipid molecules. Among them, fluorescence-quenching measurements by doxyl-labeled phospholipids, using the "parallax method", have suggested that W187 was located in the lipid bilayer, close to the membrane surface (*29*). It has been claimed furthermore that the aromatic side chain of W187 was situated near the first carbon atoms of the sn-2 acyl chain, using modified phospholipids in host micelles (*31*−*33*). The quantitative estimation of the quencher−chromophore interdistance by spin-labeled phospholipids is however limited by several factors. In particular, these reagents are not strictly contact quenchers but rather short-range quenchers (*63*−*66*). The fluctuations in the vertical direction of the unlabeled and of the doxyl-labeled phospholipids have also to be taken into account (*67*). Perhaps the most severe drawback of the estimation of the depth of a fluorophore inside a membrane bilayer using these spin-labeled fatty acids or phospholipids arises from the distortion of the acyl chain conformation by its substitution with the bulky polar doxyl group. Energy minimization calculations show that a kink is formed at the level of the substituent (not shown). In the case of the C5-labeled derivative, this leads to a location of the doxyl group at the same level as the phosphocholine polar headgroup. Moreover, results obtained in C12E8 micelles should be treated with caution since they may reflect the specific case of the host micelles of the surfactant, which has been used for these studies (*31*−*33*). Surfactant micelles in water are not quite similar to bilayer membranes especially concerning their dynamics. The packing forces of the polar headgroups are weaker in the surfactant micelle systems than in the phospholipid bilayer. This may favor the ability of surfactant molecules to penetrate the protein crevices more readily than phospholipid molecule (*68*).

The influence of the W187 residue on the binding of the protein to lipidic membranes was recently checked with a mutant lacking this residue (*69*). The effect of the mutant protein on the self-quenching of NBD-PS, used as a binding test, appeared less pronounced than that of the wild-type protein. This could however be interpreted either by a weaker binding of the protein or by a lower number of affected PS molecules. The second binding test, involving a blood coagulation assay, did not show any significant difference between the wild-type protein and the W187 mutant (*69*).

In our opinion, an important feature of the model proposed by Swairjo et al. (*14*) concerns the mobility of the W187 residue and the flexibility of domain III in the complex of annexin V with the membrane. In this model, the mobility of W187 as well as the local flexibility should be strongly reduced in the complex as compared to that of the free protein in the conformation where the calcium is bound to domain III. We have therefore measured the effect of the binding of the protein to the membrane on the W187 mobility and reexamined in more detail the interpretation of the changes of the steady-state fluorescence data brought about by interaction of annexin V with membranes, in the light of time-resolved data.

Our interpretation of the change of the fluorescence parameters upon membrane binding of annexin V is based on the three-dimensional structure in its different forms. Quenching interactions are released in the protein membrane-bound form (as in the calcium-bound form in domain III) and dipolar interactions are stronger in the new environment. These quenching interactions involve most likely the carbonyl group of Thr224, which is H-bonded to the nitrogen atom of the indole ring. Such an interaction has been shown to be strongly efficient for decreasing the fluorescence yield by an electron-transfer mechanism, the peptide bond being an electron acceptor (*70*). Time-resolved fluorescence measurements (this work and *35*) clearly show that the increase in quantum yield of W187 upon protein binding to the membrane, is in fact due to the appearance of a new long excited-state lifetime that does not exist in the unbound state of the protein. This is similar as in the calcium-bound form (*34*, *36*). This unquenched lifetime population characterizes the new conformation in which W187 is exposed to the protein surface, with no interaction with proteinaceous quencher groups.

These measurements also suggest a heterogeneity of conformations of the W187 environment, giving rise to a composite lifetime distribution coupled to a dynamic heterogeneity. In the membrane-free form of the protein at neutral pH, the short lifetime is associated with a fast subnanosecond motion while the major lifetime is associated with the Brownian motion of the protein. This pattern is not due to a macroscopic heterogeneity of the protein, which has been checked by HPLC, and which exhibits a single Brownian rotational correlation time of ∼15 ns, fully compatible with a monomer. This lifetime heterogeneity is more likely due to the coexistence of conformers in slow exchange where the indole ring is submitted to different rotational constraints. The short-lived excited-state population corresponds to a "relaxed" conformer where no rotational barriers are present, whereas the major longer-lived excited-state population is subjected to rotational hindrances and corresponds to a "tight" conformer. The existence of these different conformers can be due to slow "breathing" motions of helices in domain III, leading to flexibility of the IIIA-B loop where the W187 residue is located. Such breathing motions are suggested by molecular dynamic calculations (Sopkova et al., manuscript in preparation). In the case of the membrane-bound protein at high L/P values, a similar lifetime heterogeneity and coupling between lifetimes and correlation times are found. The flexibility of domain III is therefore preserved or even enhanced in the membrane-bound form of the protein, since nanosecond depolarization motions, that were not seen in the unbound protein, are now observable. This is also the case in reverse micelles.

From these results, we therefore suggest that W187 be probably not inserted into the membrane bilayer. It remains in the hydration water layer of the membrane, which extends some 5−6 Å from the molecular membrane surface, i.e., the thickness of two-three water layers, where the diffusion of small molecules such as acrylamide can be slowed. The reduction of the relaxation rate of local dipoles would explain the shift of the fluorescence spectrum with respect to bulk water. The interactions of domains I and II of annexin V appear stronger than those of domain III and IV according to the mutation experiments mentioned above (*40*) and also from parallel studies of binding enthalpies and intrinsic fluorescence changes (*28*) but our studies cannot give information on this point. The insertion of a Trp residue

in each of the calcium sites of the protein might provide such an answer. Furthermore, annexins I and II, which have a K instead of a W in domain III, bind to phospholipid vesicles with equal or better affinity than annexin V (*71*).

The deduced location of domain III, not in intimate contact with the membrane surface, is in agreement with recently proposed models of membrane bound annexin V using supported bilayer systems. The protein forms trimers both in crystals and on the phospholipid surface used for 2D electron microscopy analysis (*72*). The common trimer is organized with domain II situated in its center. It is stabilized by a few complementary contacts between domains I on one side and domains II and III on the other. The domains III then lie on the exterior of this common trimer. If the interaction of annexin V with the membrane surface involves the formation of this trimer as a basic unit, then the most external domains III and IV would indeed seem less crucial to this interaction. Furthermore, they could be more flexible, thus allowing the adaptation of the trimer on the membrane surface. A movement of domain III upon membrane binding has been suggested from 3D reconstruction of electron microscopy images at 16 Å resolution (*26*) and in projection at 8 Å resolution (*73*). Very recently, atomic force microscopy (AFM) measurements have suggested that the protein attaches more strongly to the membrane by domain II. This domain was less visible in the AFM images, which suggested that this domain was closer to the membrane surface than the other domains. This has the important consequence that in these supported bilayers, the convex shape of the soluble form of the protein (*10*, *13*, *14*) seems to be preserved to some extent at the membrane surface (*74*). Domain III does not seem to be close to the membrane surface. These results are at variance with the proposed three-dimensional structure calculated from negatively stained electron microscopy data, in which domain II was proposed to be the furthest from the membrane surface, whereas domain III was the nearest (*26*).

The time-resolved fluorescence experiments reported in the present work allow to refine the interpretations of the steady-state fluorescence changes that are observed upon annexin V binding to phospholipid membrane, in a more clear-cut way. They also allow the proposition of a model of the protein conformation on the membrane surface. In the membrane-bound state of the protein and in reverse micelles, the W187 environment, in terms of polarity and quenching interactions, is quite similar to that observed in the presence of calcium only and significantly more polar than that inside the protein interior at neutral pH. A conformational change bringing the W187 on the surface of the protein molecule, where it is more mobile, is therefore induced in both membrane systems. Mild acidic pH conditions were recently shown to induce the same changes both in the polarity of the W187 environment (*37*, *38*) and in the local dynamics of domain III (*38*). This suggests that the balance of a few specific electrostatic interactions is important in the conformation and dynamics of this domain in different protein environments. Such a conclusion was also reached in molecular simulation studies (Sopkova et al., manuscript in preparation). These interactions may be weakened in mild acidic pH conditions, at the membrane surface and in reverse micelles, where the proton activity, and therefore, the p*K*s of the protein ionizable groups can be modified by several units (*75*−*77*). We can remark here that another closely related annexin molecule, annexin III, exhibits a Trp residue partially solvent-exposed in domain III, in the absence of either membranes or high calcium ion concentrations at neutral pH (*17*). The accurate examination of the respective sequences and conformations of domain III of the two homologous proteins, shows that Asp226, which forms a H-bond with Thr229, stabilizing the loop IIIC−IIID, is replaced in annexin III by a Lys. The importance of this residue in the stabilization of the "closed" conformation of domain III is also emphasized in molecular simulations of the transition between the calcium-free and calcium-bound forms (Sopkova et al., manuscript in preparation). Point mutations of a few charged residues involved in the stabilization of the loops IIIA-IIIB and IIIC−IIID in annexin V are currently performed in order to test the role of these polar residues in the conformational stability of domain III.

CONCLUSIONS

Using time-resolved fluorescence spectroscopy and especially fluorescence anisotropy data, we propose that the domain III of annexin V is probably not in strong interaction with the membrane. Contrary to earlier models of the interaction of annexin V with phospholipids, we suggest that W187 is not inserted into the membrane bilayer. It remains in the hydration water layer of the membrane that extends some 5−6 Å from the molecular membrane surface, i.e., the thickness of two-three water layers.

The conformational change observed upon binding of the protein to the membrane is most likely the same as the one induced by higher calcium concentrations in the absence of membrane systems, by mild acidic pH conditions and the incorporation into reverse micelles. The mechanism of this conformational change at the membrane surface involves probably a shift of the apparent p*K*(s) of specific ionizable acidic group(s). This is likely to occur in the membrane hydration layer and also in reverse micelles, due to the increase of the proton activity in the membrane/water interfacial region (*77*). This may facilitate the conformational change of domain III on the membrane surface at low calcium concentrations.

ACKNOWLEDGMENT

We are very grateful to Dr. I. Maurer-Fogy (Bender and Co., Vienna, Austria) for a generous gift of pure recombinant human annexin V. The technical staff of LURE is acknowledged for running the synchrotron facility during the beam sessions.

REFERENCES

1. Meers, P. (1996) in *Annexins: Molecular Structure to Cellular Function* (Seaton, B. A., Ed.) Chapter 8, pp 97−119, Chapman and Hall, New York.
2. Gerke, V., and Moss, S. E. (1997) *Biochim. Biophys. Acta 1357*, 129−154.
3. Raynal, P., and Pollard, H. B. (1994) *Biochim. Biophys. Acta 1197*, 63−93.
4. Swairjo, M. A., and Seaton, B. A. (1994) *Annu. Rev. Biophys. Biomol. Struct. 23*, 193−213.
5. Hollenberg, M. D., Valentine-Braun, K. A., and Northup, J. (1988) *Trends Pharm. Sci. 9*, 63−66.
6. Creutz, C. E. (1992) *Science 258*, 924−931.
7. Huang, K. S., Wallner, B. P., Mattaliano, R. J., Tizard, R., Burne, C., Frey, A., Hession, C., McGray, P., Sinclair, L. K., Chow, E. P., Browning, J. L., Ramachandran, K. L., Tang, J., Smart, J. E., and Pepinski, R. B. (1986) *Cell 46*, 191−199.

8. Geisow, M. J., Walker, J. H., Boustead, C., and Taylor, W. (1987) *Biosci. Rep. 7*, 289−298.
9. Glenney, J. R., Jr. (1986) *J. Biol. Chem. 261*, 7247−7252.
10. Huber R., Römisch J., and Paques E. P. (1990) *EMBO J. 9*, 3867−3874.
11. Concha, N. O., Head, J. F., Kaetzel, M. A., Dedman, J. R., and Seaton, B. A. (1993) *Science 261*, 1321−1324.
12. Lewit-Bentley, A., Morera, S., Huber, R., and Bodo, R. (1992) *Eur. J. Biochem. 210*, 73−77.
13. Sopkova, J., Renouard, M., and Lewit-Bentley, A. (1993) *J. Mol. Biol. 234*, 816−825.
14. Swairjo, M. A., Concha, N. O., Kaetzel, M. A., Dedman, J. R., and Seaton, B. A. (1995) *Nat. Struct. Biol. 2*, 968−974.
15. Weng, X., Luecke, H., Song, I. S., Kang, D. S., Kim, S. H., and Huber, R. (1993) *Protein Sci. 2*, 448−458.
16. Luecke, H., Chang, B. T., Maillard, W. S., Schlaepfer, D. D., and Haigler, H. T. (1995) *Nature 378*, 512−515.
17. Favier-Perron, B., Lewit-Bentley, A., and Russo-Marie, F. (1996) *Biochemistry 35*, 1740−1744.
18. Burger, A., Berendes, R., Liemann, S., Benz, J., Hofmann, A., Göttig, P., Huber, R., Gerke, V., Thiel, C., Römisch, J., and Weber, J. (1996) *J. Mol. Biol. 257*, 839−847.
19. Benz, J., Bergner, A., Hofmann, A., Demange, P., Göttig, P., Liemann, S., Huber, R., and Voges, D. (1996) *J. Mol. Biol. 260*, 638−643.
20. Kawasaki, H., Avilasakar, A., Creutz, C. E., and Kretzinger, R. H. (1996) *Biochim. Biophys. Acta 1313*, 277−282.
21. Liemann, S., Bringemeier, I., Benz, J., Göttig, P., Hofmann, A., Huber, R., Noegel, A. A., and Jacob, U. (1997) *J. Mol. Biol. 270*, 79−88.
22. Zanotti, G., Malpeli, G., Gliubich, F., Folli, C., Stoppini, M., Olivi, L., Savoia, A., and Berni, R. (1998) *Biochem. J. 329*, 101−106.
23. Berendes, R., Voges, D., Demange, P., Huber, R., and Burger, A. (1993) *Science 262*, 427−430.
24. Brisson, A., Mosser, G., and Huber, R. (1991) *J. Mol. Biol. 220*, 199−203.
25. Pigault, C., Follenius-Wund, A., Schmutz, M., Freyssinet, J.-M., and Brisson, A. (1994) *J. Mol. Biol. 236*, 199−208.
26. Voges, D., Berendes, R., Burger, A., Demange, P., Baumeister, W., and Huber, R. (1994) *J. Mol. Biol. 238*, 199−213.
27. Concha, N. O., Head, J. F., Kaetzel, M. A., Dedman, J. R., and Seaton, B. A. (1992) *FEBS Lett. 314*, 159−162.
28. Plager, D. A., and Nestuelen, G. L. (1994) *Biochemistry 33*, 13239−13249.
29. Meers, P. (1990) *Biochemistry 29*, 3325−3330.
30. Meers, P., Bentz, J., Alford, D., Nir, S., Papahadjopoulos, D., and Hong, K. (1988) *Biochemistry 27*, 4430−4439.
31. Meers, P., and Mealy, T. R. (1993) *Biochemistry 32*, 5411−5418.
32. Meers, P., and Mealy, T. R. (1993) *Biochemistry 32*, 11711−11721.
33. Meers, P., and Mealy, T. R. (1994) *Biochemistry 33*, 5829−5837.
34. Sopkova, J. (1994) Ph.D. Thesis, Universities of Prague and Orsay.
35. Follenius-Wund, A., Piémont, E, Freyssinet, J.-M., Gérard, D., and Pigault, C. (1997) *Biochem. Biophys. Res. Commun. 234*, 111−116.
36. Sopkova, J., Gallay, J., Vincent, M., Pancoska, P., and Lewit-Bentley, A. (1994) *Biochemistry 33*, 4490−4499.
37. Beermann, Br. B., Hinz, H.-J., Hofmann, A., and Huber, H. (1998) *FEBS Lett. 423*, 265−269.
38. Sopkova, J., Vincent, M., Takahashi, M., Lewit-Bentley, A., and Gallay, J. (1998) *Biochemistry 37*, 11962−11970.
39. Saurel, O., Cezanne, L., Milon, A., Tocanne, J. F., and Demange, P. (1998) *Biochemistry 37*, 1403−1410.
40. Cordier-Ochsenbein, F. (1997) Ph.D. Thesis, University Paris-Sud, Orsay, France.
41. Meers, P., Daleke, D., Hong, K., and Papahadjopoulos, D. (1991) *Biochemistry 30*, 2903−2908.
42. Luisi, P. L., and Magid, L. J. (1986) *Crit. Rev. Biochem. 20*, 409−474.
43. Waks, M. (1986) *Proteins: Struct., Funct., Genet. 1*, 4−15.
44. Maurer-Fogy, I., Reutelingsperger, C. P. M., Peiters, J., Bodo, G., Stratowa, C., and Hauptman, R. (1988) *Eur. J. Biochem. 174*, 585−592.
45. Gallay, J., Vincent, M., Nicot, C., and Waks, M. (1987) *Biochemistry 26*, 5738−5747.
46. Rouvière, N., Vincent, M., Craescu, C. T., and Gallay, J. (1997) *Biochemistry 36*, 7339−7352.
47. Vincent, M., Gallay, J., and Demchenko, A. P. (1995) *J. Phys. Chem. 99*, 14931−14941.
48. Brochon, J.-C. (1994) *Methods in Enzymol. 240*, 262−311.
49. Vincent, M., Brochon, J.-C., Mérola, F., Jordi, W., and Gallay, J. (1988) *Biochemistry 27*, 8752−8761.
50. Kinosita, K., Kawato, S., and Ikegami, A. (1977) *Biophys. J. 20*, 289−305.
51. Eftink, M. (1991) in *Topics in Fluorescence Spectroscopy vol. 2 Principles* (Lakowicz, J. R., Ed.) Chapter 2, pp 53−126, Plenum Press, New York.
52. Spencer, R. D., and Weber, G. (1970) *J. Chem. Phys. 52*, 1654−1663.
53. Valeur, B., and Weber, G. (1977) *Photochem. Photobiol. 25*, 441−444.
54. Gallay, J., Vincent, M., Li de la Sierra, I. M., Alvarez, J., Ubieta, R., Madrazo, J., and Padrón, G. (1993) *Eur. J. Biochem. 211*, 213-219.
55. Marzola, P., and Gratton, E. (1991) *J. Phys. Chem. 95*, 9488−9495.
56. Lentz, V. L., Federwisch, M., Gattner, H.-G., Brandenburg, D., Höcker, H., Hassiepen, U., and Wollmer, A. (1995) *Biochemistry 34*, 6130−6141.
57. Visser, A. J. W. G. (1997) *Curr. Opin. Colloid Interface Sci. 2*, 27−36.
58. Dijkstra, B. W., Kalk, K. H., Hol, W. G. J., and Drenth, J. (1981) *J. Mol. Biol. 147*, 97−123.
59. Huber, R., Berendes, R., Burger, A., Schneider, M., Karshikov, A., Luecke, H., Romisch, J., and Paques, E. P. (1992) *J. Mol. Biol. 223*, 683−704.
60. Voges, K.-P., Jung, G., and Sawyer, W. H. (1987) *Biochim. Biophys. Acta 896*, 64−76.
61. Callis, P. R. (1997) *Methods Enzymol. 278*, 113−150.
62. Swairjo, M. A., Roberts, M. F., Campos, M.-A., Dedman, J. R., and Seaton, B. A. (1994) *Biochemistry 33*, 10944−10950.
63. Green, J. A., Singer, L. A., and Parks, J. H. (1973) *J. Chem. Phys. 58*, 2690.
64. London, E., and Feigenson, G. W. (1981) *Biochemistry 20*, 1932−1938.
65. Chattopadhyay, A., and London, E. (1987) *Biochemistry 26*, 39−45.
66. Yeager M. D., and Feigenson, G. W. (1990) *Biochemistry 29*, 4380−4392.
67. Ladokhin, A. S., and Holloway, P. W. (1995) *Biophys. J. 69*, 506−517.
68. Tanford, C., and Reynolds, J. A. (1976) *Biochim. Biophys. Acta 457*, 133−170.
69. Campos, B., Mo, Y. D., Mealy, T. R., Swairjo, M. A., Balch, C., Head, J. F., Retzinger, G., Dedman, J. R., and Seaton, B. A. (1998) *Biochemistry 37*, 8004−8010.
70. Chen, Y., Liu, B., Hong-Tao, Y., and Barkley, M. D. (1996) *J. Am. Chem. Soc. 118*, 9271−9278.
71. Blackwood, R. A., and Ernst, J. D. (1990) *Biochem. J. 266*, 195−200.
72. Brisson, A., and Lewit-Bentley, A. (1996) in *Annexins: Molecular Structure to Cellular Function* (Seaton, B. A., Ed.), Chapter 4, pp 43−52, Chapman and Hall, New York.
73. Olofsson, A., Mallouh, V., and Brisson, A. (1995) *J. Struct. Biol. 113*, 199−205.
74. Reviakine, I., Bergma-Schutter, W., and Brisson, A. (1998) *J. Struct. Biol. 121*, 356−361.
75. El Seoud, O. A. (1984) in *Reverse Micelles* (Luisi, P. L., and Straub, B. E., Eds.) pp 81−93, Plenum Press, New York.
76. Hauser, H., and Shipley, G. G. (1985) *Biochim. Biophys. Acta 813*, 343−346.
77. Teissié, J., Prats, M., Soucaille, P., and Tocanne, J. F. (1985) *Proc. Natl. Acad. Sci. U.S.A. 82*, 3217−3221.

BI982760G